TÜBİTAK

Turk J Elec Eng & Comp Sci, Vol.20, No.3, 2012, © TÜBİTAK
doi:10.3906/elk-1007-596

Reduction of torque ripple in DTC for induction motor using input-output feedback linearization

Sebti BELKACEM*, Farid NACERI, Rachid ABDESSEMED
Department of Electrical Engineering, University of Batna, Batna-ALGERIA
e-mail: belkacem_sebti@yahoo.fr

Received: 31.10.2010

Abstract

Direct torque control (DTC) is known to produce fast responses and robust control in AC adjustable-speed drives. However, in the steady-state operation, notable torque, flux, and current pulsations occur. In this paper, nonlinear DTC of induction motor drives is presented based on a space vector pulse-width modulation scheme combined with the input-output feedback linearization technique. The variation of stator and rotor resistance due to changes in temperature or frequency deteriorates the performance of the DTC controller by introducing errors in the estimated flux linkage and the electromagnetic torque. This approach will not be suitable for high power drives such as those used in tractions, as they require good torque control performance at a considerably lower frequency. Finally, extensive simulation results are presented to validate the proposed technique. The system is tested at different speeds and a very satisfactory performance is achieved.

Key Words: *Direct torque control with space vector pulse-width modulation, key parameter variations, robustness, input-output feedback linearization*

1. Introduction

Today, direct torque control (DTC) and nonlinear control (NLC) are considered the most important techniques for achieving high dynamic performance in AC machines. The DTC scheme has grown due to several factors, such as quick torque response and robustness against the motor parameter variations [1]. The conventional DTC algorithm using the hysteresis-based voltage switching method has the relative merits of a simple structure and easy implementation. The performance of such a scheme depends on the error band set between the desired and measured torque and stator flux values. In addition, in this control scheme, the inverter switching frequency is changed according to the hysteresis bandwidth of the flux and torque controllers and the variation of the speed and motor parameters. Superior motor performance is achieved by narrower hysteresis bands, especially in the high speed region.

To overcome the technique's drawbacks, several methods have been presented. DTC with space vector modulation (SVM) is based on the deadbeat control derived from the torque and stator flux errors. It offers

*Corresponding author: Department of Electrical Engineering, University of Batna, Batna-ALGERIA

good steady-state and dynamic performances with reduction in the phase current distortion and fast torque response. However, this technique has limitations in being computationally intensive [2-5].

In recent works [6,7], modified direct torque and flux control schemes were proposed based on sliding-mode control (SMC). It is well known that the sliding-mode controller rejects perturbations that verify the matching conditions. This important feature of robustness makes the controller suitable for this application in order to overcome parameter mismatches. The drawback of this combination (DTC-SMC) is that using the saturation function introduces a persistent static error and the need for knowledge of the dynamics of the system.

A control technique [8] was developed for matrix converters that generates, under unity input power factor conditions, the voltage vectors needed to implement the DTC for induction motors. The switching state of the matrix converter is selected from a matrix-switching table, which was developed based on a conventional voltage source inverter switching table.

Fuzzy logic controllers have been used in DTC systems in the past few years. In [9-11], a fuzzy logic controller was used to select voltage vectors in conventional DTC. For the duty ratio control method, a fuzzy logic controller is used to determine the duration of the output voltage vector at each sampling period.

The adaptive neural fuzzy inference system method is based on fuzzy logic and artificial neural networks for decoupled stator flux and torque control. The stability will be affected by parameter variation and the system model must be known, as the system's dynamic performance and stability will be significantly affected by parameter variations [12].

To solve this problem, adaptive nonlinear control methods such as the adaptive input-output feedback linearization (IOFL) technique, adaptive backstepping control technique, and sliding-mode and adaptive SMC techniques have been applied to induction motor (IM) drives [13-24]. In those studies, an adaptation law was developed to compensate for the parametric uncertainty of the stator and rotor resistance and the external load torque of the IM. The contribution of this paper is to describe a robust DTC with space vector pulse-width modulation (DTC-SVPWM) method for torque and flux control of an IM drive based on the IOFL technique. Simulation results demonstrate the feasibility and validity of the proposed DTC system in effectively accelerating the system response, reducing torque and flux ripple, and achieving a very satisfactory performance.

2. IM model

The model of the IM expressed in the stationary "$\alpha\beta$" axes reference frame can be described by [13]:

$$\begin{aligned}
\frac{d\,i_{s\alpha}}{dt} &= -(\frac{R_s}{\sigma L_s}+\frac{R_r}{\sigma L_r})i_{s\alpha}-\omega_r i_{s\beta}+\frac{R_r}{\sigma L_r L_s}\Phi_{s\alpha}+\frac{\omega_r}{\sigma L_s}\Phi_{s\beta}+\frac{1}{\sigma L_s}V_{s\alpha},\\
\frac{d\,i_{s\beta}}{dt} &= -(\frac{R_s}{\sigma L_s}+\frac{R_r}{\sigma L_r})i_{s\beta}+\omega_r i_{s\alpha}+\frac{R_r}{\sigma L_r L_s}\Phi_{s\beta}-\frac{\omega_r}{\sigma L_s}\Phi_{s\alpha}+\frac{1}{\sigma L_s}V_{s\beta},\\
\frac{d\,\Phi_{s\alpha}}{dt} &= V_{s\alpha}-R_s i_{s\alpha},\\
\frac{d\,\Phi_{s\beta}}{dt} &= V_{s\beta}-R_s i_{s\beta}.
\end{aligned} \tag{1}$$

Here, i_s, Φ_s, V_s, R, and L denote stator currents, stator flux, stator voltage, resistance, and inductance, respectively, ω_r denotes the rotor speed, and M is the mutual inductance. $\sigma = 1-\frac{M^2}{L_s L_r}$ is the redefined leakage inductance.

The generated torque of the IM can be expressed in terms of stator currents and stator flux linkage as:

$$T_e = \frac{3p}{2}(\Phi_{s\alpha} i_{s\beta} - \Phi_{s\beta} i_{s\alpha}), \tag{2}$$

where p is the number of pole pairs.

The mechanical dynamic equation is given by:

$$\frac{d\omega_m}{dt} = \frac{3p}{2J}(\Phi_{s\alpha} i_{s\beta} - \Phi_{s\beta} i_{s\alpha}) - \frac{T_L}{J}, \tag{3}$$

where J and T_L denote the moment of inertia of the motor and the load torque, and ω_m is the rotor mechanical speed ($\omega_r = p\omega_m$).

For the proposed nonlinear IOFL controller, the state coordinate transformation is applied. Therefore, the state coordinate's transformed model from Eq. (1) can be rewritten in a compact form as [18]:

$$\dot{x} = f(x) + g_1(x).V_{s\alpha} + g_2(x).V_{s\beta}, \tag{4}$$

$$y = h(x),$$

where x is defined as:

$$f(x) = \begin{bmatrix} -(\frac{R_s}{\sigma L_s} + \frac{R_r}{\sigma L_r})i_{s\alpha} - \omega_r i_{s\beta} + \frac{R_r}{\sigma L_r L_s}\Phi_{s\alpha} + \frac{\omega_r}{\sigma L_s}\Phi_{s\beta} \\ -(\frac{R_s}{\sigma L_s} + \frac{R_r}{\sigma L_r})i_{s\beta} + \omega_r i_{s\alpha} + \frac{R_r}{\sigma L_r L_s}\Phi_{s\beta} - \frac{\omega_r}{\sigma L_s}\Phi_{s\alpha} \\ -R_s i_{s\alpha} \\ -R_s i_{s\beta} \end{bmatrix}, \tag{5}$$

$$x = [i_{s\alpha}, i_{s\beta}, \Phi_{s\alpha}, \Phi_{s\beta}]^T, g_1(x) = \begin{bmatrix} \frac{1}{\sigma L_s} & 0 & 1 & 0 \end{bmatrix}^T g_2(x) = \begin{bmatrix} 0 & \frac{1}{\sigma L_s} & 0 & 1 \end{bmatrix}^T. \tag{6}$$

At this stage, the generated torque, T_e, and the squared modules of the stator flux linkage, $|\Phi_s|^2 = \Phi_{s\alpha^2} + \Phi_{s\beta^2}$, are assumed to be the system outputs. Therefore, by considering:

$$\begin{aligned} h_1(x) = T_e &= \tfrac{3p}{2}(\Phi_{s\alpha} i_{s\beta} - \Phi_{s\beta} i_{s\alpha}), \\ h_2(x) = |\Phi_s|^2 &= \Phi_{s\alpha^2} + \Phi_{s\beta^2}, \end{aligned} \tag{7}$$

controller objectives y_1 and y_2 can be defined as:

$$\begin{aligned} y_1 &= h_1(x), \\ y_2 &= h_2(x). \end{aligned} \tag{8}$$

3. Input-output feedback linearization

For the linearization of the nonlinear model in Eq. (4), the controlled variable is differentiated with respect to time until the input appears. This can be easily done by introducing the Lie derivative.

3.1. Lie derivatives

Consider the system in Eq. (4). Differentiating output y with respect to time yields [19]:

$$\dot{y} = \frac{\partial h}{\partial x}\dot{x} = \frac{\partial h}{\partial x}\left[f(x) + g(x)V\right] = L_f h(x) + L_g h(x)V, \tag{9}$$

where $L_f h(x) = \frac{\partial h}{\partial x} f(x), L_g h(x) = \frac{\partial h}{\partial x} g(x)$.

The function $L_f h(x)$ is called the Lie derivative of $h(x)$ with respect to $f(x)$, and it corresponds to the derivative of h along the trajectories of the system $\dot{x} = f(x)$. Similarly, $L_g h(x)$ is called the Lie derivative of h with respect to g, and it corresponds to the derivative of function $h(x)$ along the trajectories of the system $\dot{x} = g(x)$.

3.2. Relative degree of a nonlinear system

For nonlinear systems, the relative degree r of the system in Eq. (4) corresponds to the number of times the output $y = h(x)$ has to be differentiated with respect to time before input u appears explicitly in the resulting equations.

The system in Eq. (4) is said to have a relative degree r, $1 \leq r \leq n$ in R^n if $\forall x \in R^n$:

$$\begin{aligned} &L_g L_f^{i-1} h(x) = 0 \quad i = 1, 2, ..., r-1, \\ &L_g L_f^{r-1} h(x) \neq 0, \end{aligned} \tag{10}$$

where $L_g L_f^i h(x) = L_g\left[L_f^i h(x)\right], L_f^i h(x) = L_f\left[L_f^{i-1} h(x)\right], i = 1, 2, ..., r-1$

and $L_f^0 h(x) \triangleq h(x)$.

Using the above notation, we can obtain the relative degree.

3.2.1. Relative degree of the torque

$$\dot{y}_1 = L_f h_1(x) + L_{g1} h_1(x) V_{s\alpha} + L_{g2} h_1(x) V_{s\beta} = \frac{\partial h_1}{\partial x} f(x) + \frac{\partial h_1}{\partial x} g_1(x).V_{s\alpha} + \frac{\partial h_1}{\partial x} g_2(x).V_{s\beta}, \tag{11}$$

with

$$L_f h_1 = -\frac{3p}{2}\Phi_{s\beta}\left[-(\frac{R_s}{\sigma L_s} + \frac{R_r}{\sigma L_r})i_{s\alpha} - \omega_r i_{s\beta} + \frac{\omega_r}{\sigma L_s}\Phi_{s\beta}\right] + \frac{3p}{2}\Phi_{s\alpha}\left[-(\frac{R_s}{\sigma L_s} + \frac{R_r}{\sigma L_r})i_{s\beta} + \omega_r i_{s\alpha} - \frac{\omega_r}{\sigma L_s}\Phi_{s\alpha}\right],$$

$$L_{g1} h_1 = \frac{3p}{2}(i_{s\beta} - \frac{1}{L_s \sigma}\Phi_{s\beta}),$$

$$L_{g2} h_1 = \frac{3p}{2}\left(\frac{1}{L_s \sigma}\Phi_{s\alpha} - i_{s\alpha}\right).$$

The relative degree of $\mathrm{y}_1(\mathrm{x})$ is $\mathrm{r}_1 = 1$.

3.2.2. Relative degree of the flux

$$\dot{y}_2 = L_f h_2(x) + L_{g1} h_2(x) V_{s\beta} + L_{g2} h_2(x) V_{s\alpha} = \frac{\partial h_2}{\partial x}.f(x) + \frac{\partial h_2}{\partial x} g_1(x).V_{s\alpha} + \frac{\partial h_2}{\partial x} g_2(x).V_{s\beta}, \tag{12}$$

with

$$L_f h_2 = -2R_s \left(\Phi_{s\alpha} i_{s\alpha} - \Phi_{s\beta} i_{s\beta}\right),$$

$$L_{g1} h_2 = 2\Phi_{s\alpha},$$

$$L_{g2} h_2 = 2\Phi_{s\beta}.$$

The relative degree of $\mathrm{y}_2(\mathrm{x})$ is $\mathrm{r}_2 = 1$.

4. Decoupling matrix

The matrix defining the relation between physical input u and output derivative y(x) is given by [20]:

$$\begin{bmatrix} \dot{y}_1 \\ \dot{y}_2 \end{bmatrix} = A(x) + E(x) \begin{bmatrix} V_{s\alpha} \\ V_{s\beta} \end{bmatrix}, \tag{13}$$

with

$$A(x) = \begin{bmatrix} L_f h_1 \\ L_f h_2 \end{bmatrix},$$

$$E(x) = \begin{bmatrix} L_{g1} h_1 & L_{g2} h_1 \\ L_{g1} h_2 & L_{g2} h_2 \end{bmatrix},$$

$$E(x) = \begin{bmatrix} \frac{3p}{2}(i_{s\beta} - \frac{1}{L_s \sigma}\Phi_{s\beta}) & \frac{3p}{2}\left(\frac{1}{L_s \sigma}\Phi_{s\alpha} - i_{s\alpha}\right) \\ 2\Phi_{s\alpha} & 2\Phi_{s\beta} \end{bmatrix}, \tag{14}$$

$$\det(E) = \frac{3p}{2}(i_{s\beta} - \frac{1}{L_s \sigma}\Phi_{s\beta}).2\Phi_{s\beta} - \frac{3p}{2}\left(\frac{1}{L_s \sigma}\Phi_{s\alpha} - i_{s\alpha}\right).2\Phi_{s\alpha} = 3p(i_{s\beta} - \frac{1}{L_s \sigma}\Phi_{s\beta}).\Phi_{s\beta} - 3p\left(\frac{1}{L_s \sigma}\Phi_{s\alpha} - i_{s\alpha}\right).\Phi_{s\alpha}, \tag{15}$$

$$\det(E) = 3p\left[-\frac{1}{L_s \sigma}(\Phi_{s\beta}^2 + \Phi_{s\alpha}^2) + i_{s\beta}\Phi_{s\beta} + i_{s\alpha}\Phi_{s\alpha}\right], \tag{16}$$

using the induction motor model of Eq. (1):

$$\begin{aligned} i_{s\alpha} &= \frac{1}{\sigma L_s}\Phi_{s\alpha} - \frac{M}{\sigma L_s L_r}\Phi_{r\alpha}, \\ i_{s\beta} &= \frac{1}{\sigma L_s}\Phi_{s\beta} - \frac{M}{\sigma L_s L_r}\Phi_{r\beta}, \end{aligned} \tag{17}$$

and linking Eqs. (16) and (17):

$$\det(E) = -3p.\frac{M}{\sigma L_s L_r}\left[\Phi_{s\beta}\Phi_{r\beta} + \Phi_{s\alpha}\Phi_{r\alpha}\right]. \tag{18}$$

It is clear that matrix E(x) is always reversible. The product of the stator flux and rotor flux cannot be equal to zero, and the following IOFL is introduced for the system given in Eq. (4):

$$\begin{bmatrix} V_{s\alpha} \\ V_{s\beta} \end{bmatrix} = E^{-1}(x) \left[-A(x) + \begin{bmatrix} V_1 \\ V_2 \end{bmatrix} \right], \tag{19}$$

where

$V = \begin{bmatrix} V_1 \\ V_2 \end{bmatrix}$, are the new inputs.

Substituting Eq. (12) into Eq. (9), the system dynamics are:

$$\begin{cases} V_1 = \dot{h}_1(x), \\ V_2 = \dot{h}_2(x). \end{cases} \tag{20}$$

To ensure perfect regulation and track the desired signals of the flux and torque toward their reference, V_1 and V_2 are chosen as follows [13]:

$$\begin{cases} V_1 = \left|\dot{\Phi}_s\right|^2_{ref} + k_1(|\Phi_s|^2_{ref} - |\Phi_s|^2), \\ V_2 = \dot{T}_{e\,ref} + k_2(T_{e\,ref} - T_e). \end{cases} \tag{21}$$

Here, the subscript 'ref' denotes the reference value and (k_1, k_2) are constant design parameters to be determined in order to make the decoupled system in Eq. (14) stable. The behavior of the linearized model is imposed by the pole placement method. The coefficients selected, such as $s + k_1$ and $s + k_2$, are the Hurwitz polynomials [19].

5. Voltage space vector PWM

The voltage vectors, produced by a 3-phase pulse-width modulation (PWM) inverter, divide the space vector plane into 6 sectors, as shown in Figure 1.

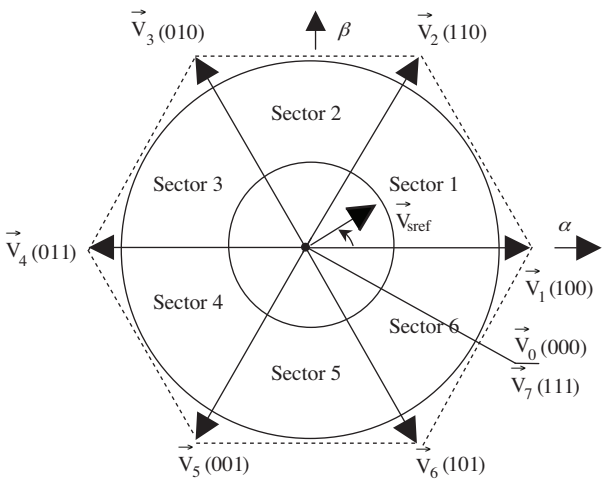

Figure 1. The diagram of voltage space vectors.

In every sector, each voltage vector is synthesized by the basic space voltage vector of the 2 sides of the sector and 1 zero vector. For example, in the first sector, $\bar{V}_{s\,ref}$ is a synthesized voltage space vector and is expressed by [2]:

$$\bar{V}_{s\,ref}T_s = \bar{V}_0T_0 + \bar{V}_1T_1 + \bar{V}_2T_2, \tag{22}$$

$$T_s = T_0 + T_1 + T_2, \tag{23}$$

where T_0, T_1, and T_2 are the work times of basic space voltage vectors $\bar{V}_0$, $\bar{V}_1$, and $\bar{V}_2$, respectively.

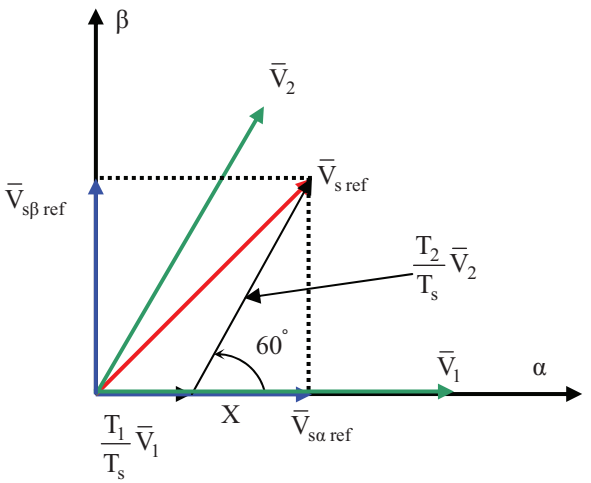

Figure 2. Projection of the reference voltage vector.

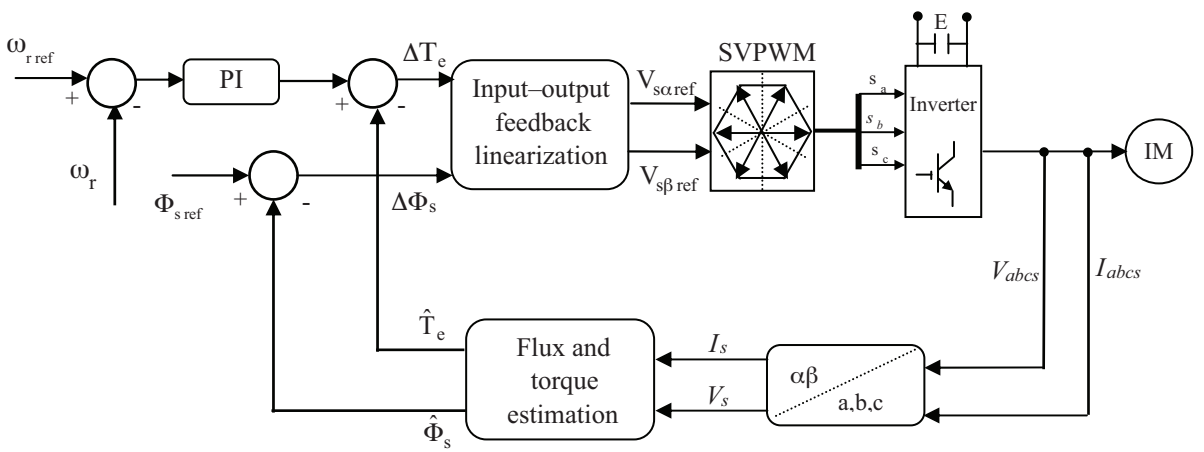

Figure 3. Block diagram of the proposed DTC based on IOFL.

6. Sensitivity study and simulation results

In this section, the effectiveness of the proposed algorithm for torque and flux control of an IM is verified by computer simulations. The block scheme of the investigated DTC-SVPWM for a voltage source inverter-fed IM

is presented in Figure 3. A series of tests were conducted to check the performance of the proposed system. In all Figures, the time axis is scaled in seconds. The coefficients of the conventional motor speed proportional-integral controller were chosen as ($K_p = 4.66$, $K_i = 77.77$).

6.1. Variation of the load torque

Figure 4 shows the speed response of classical DTC and DTC based on the IOFL controller. The DTC-IOFL reacts faster than the classical DTC when load torque is suddenly applied and removed.

Moreover, tracking performances were improved by the use of the DTC-IOFL law, in comparison with those of classical DTC. These properties make the new algorithm suitable for applications where high tracking accuracy is required in the presence of external disturbances.

Current ripple was also notable reduced in DTC-IOFL compared to classical DTC. A significantly lower ripple level in torque flux is shown in Figure 5, and Figure 6 shows the trajectory of the estimated stator flux components. The new DTC has as good of a dynamic response as the classical control.

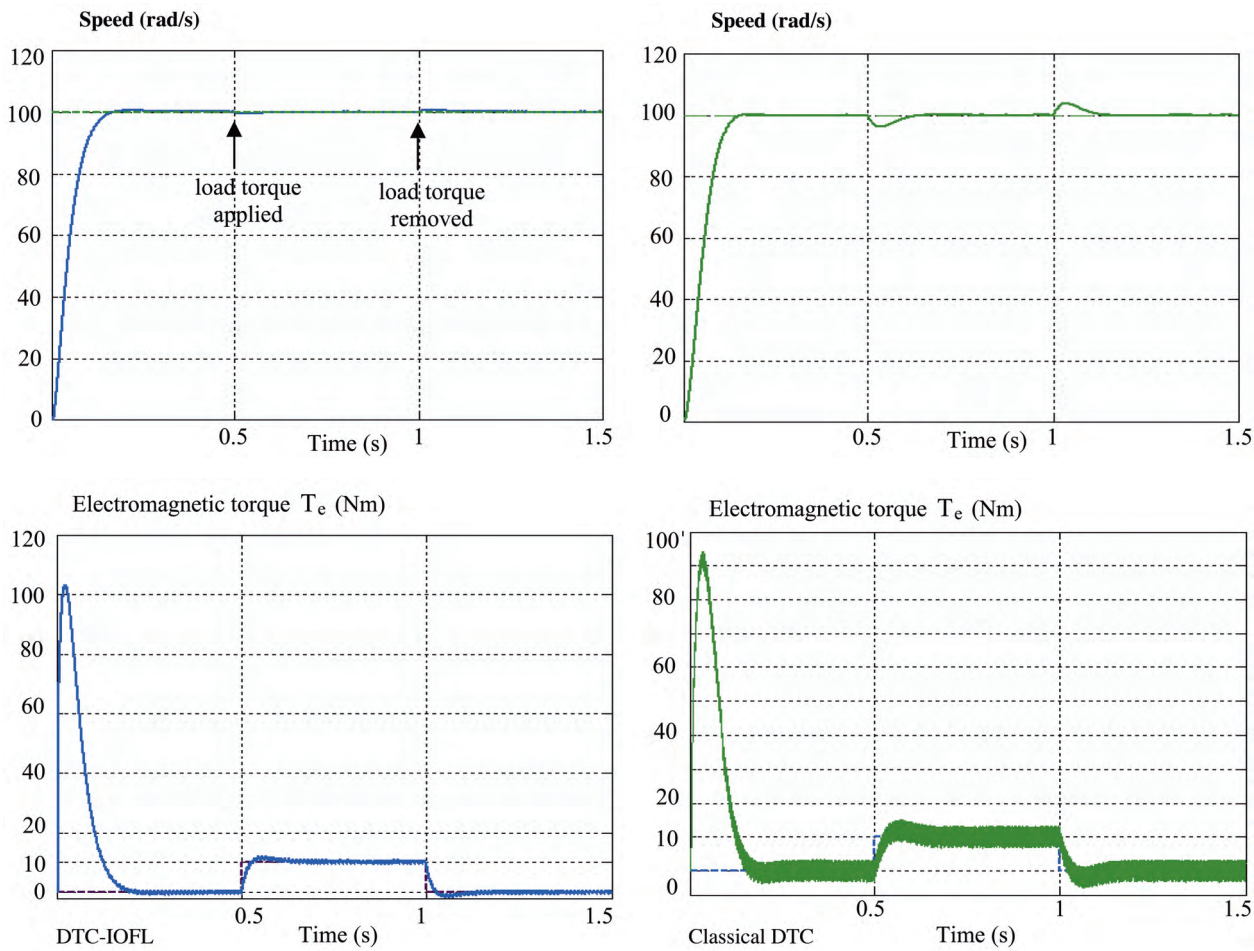

Figure 4. Drive response under load torque change.

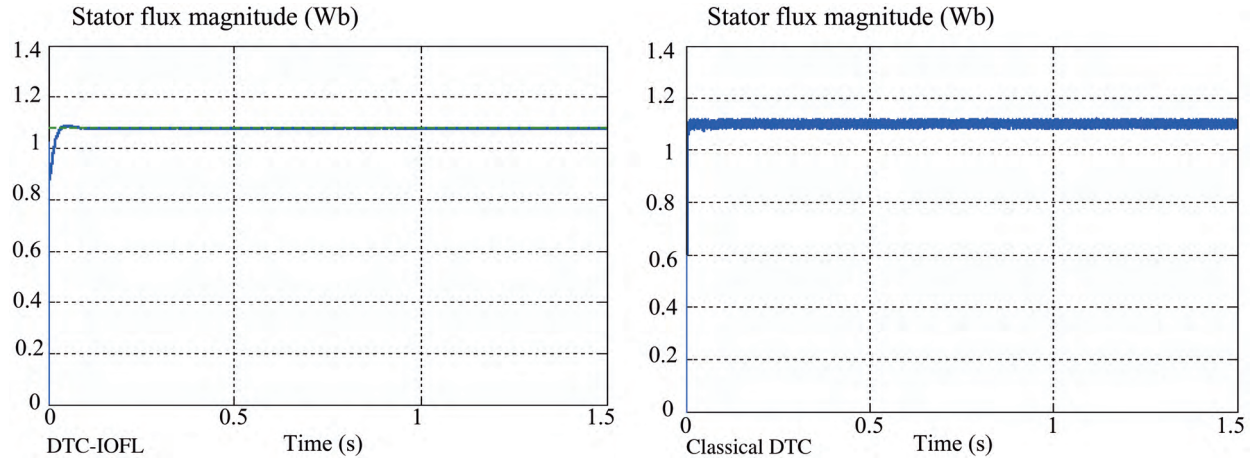

Figure 4. Continued.

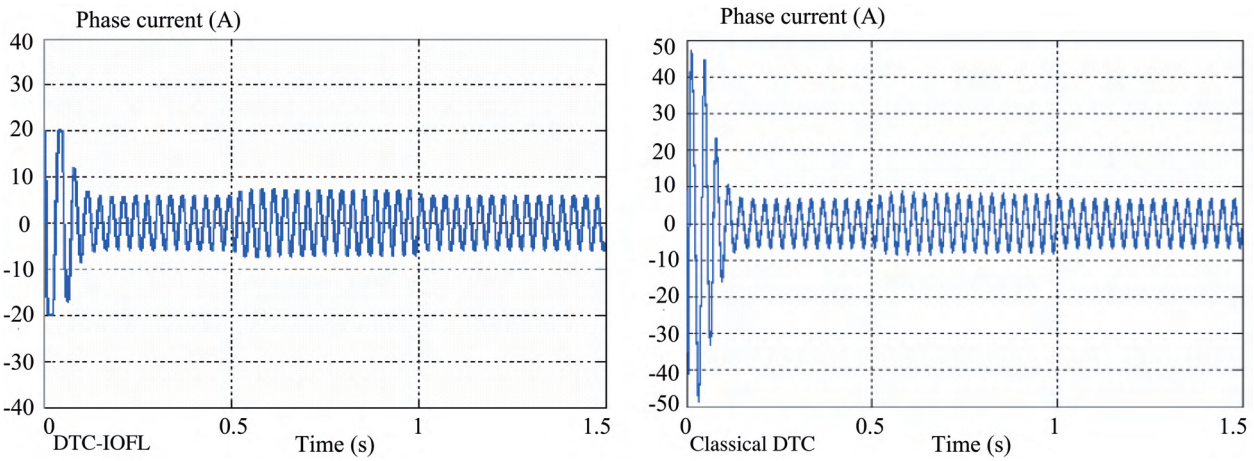

Figure 5. Drive response under load torque change.

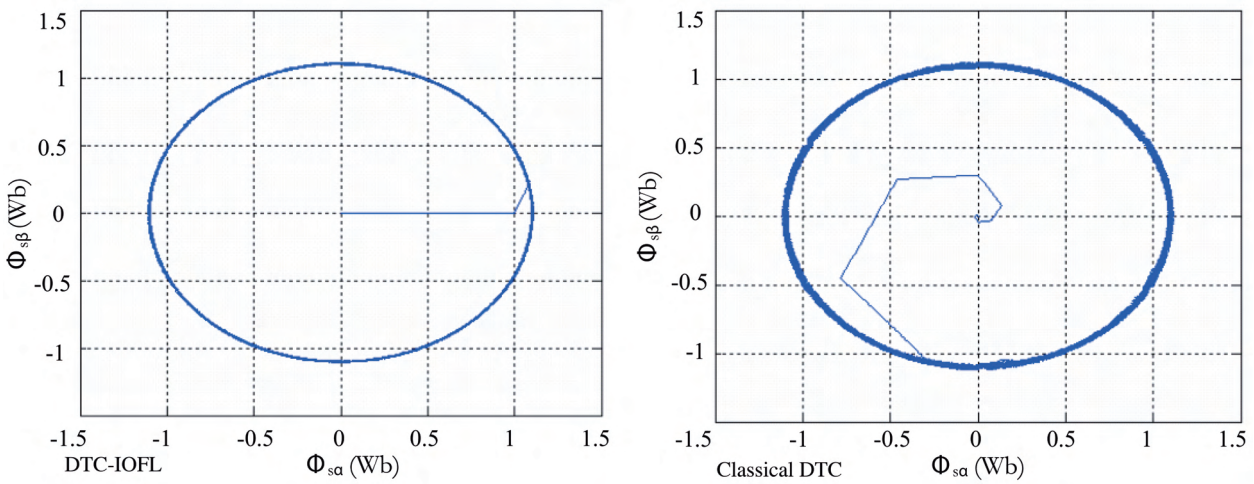

Figure 6. Drive response under load torque change.

7. Variation in the stator resistance

The influence of changes in the electrical parameters on the drive performance was investigated. Figure 7 depicts the drive performance for brusque changes in the stator resistance and illustrates the simulation results of the process of speed estimation with a speed reference equal to 30 rad/s. After R_s increases by 50% and

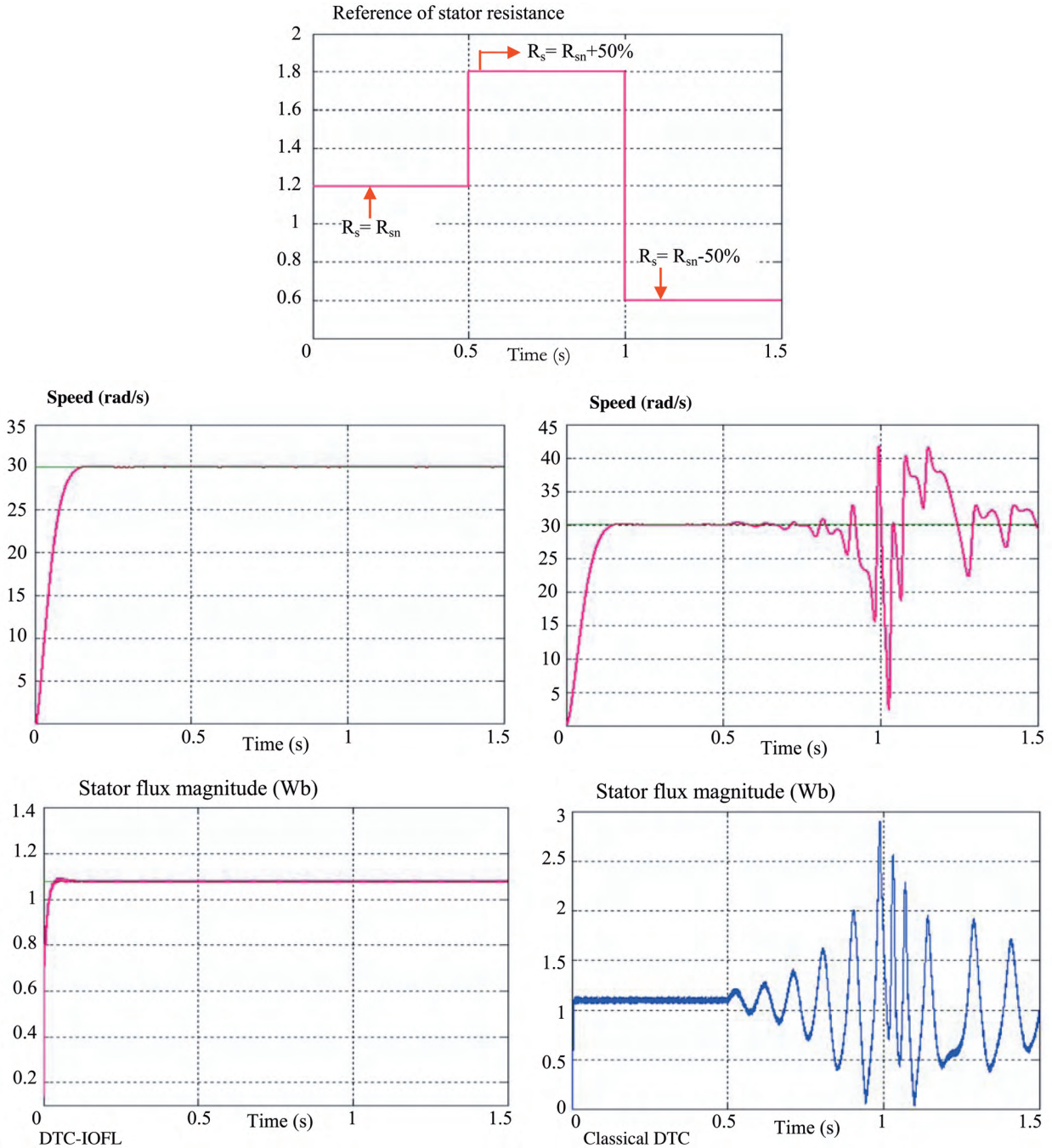

Figure 7. Drive response under stator resistance change.

decreases by 50%, the variation in the stator resistance will not affect the controller performance. In the case of DTC-IOFL, the new algorithm shows more robustness against stator resistance variation compared to classical DTC.

7.1. Variation in the inertia coefficient

Figure 8 shows the drive dynamic under different values of inertia with a constant speed reference. It is clear that the speed tracking is significantly unchanged after J increases by 50% and decreases by 50% for DTC-IOFL compared to the classical controller.

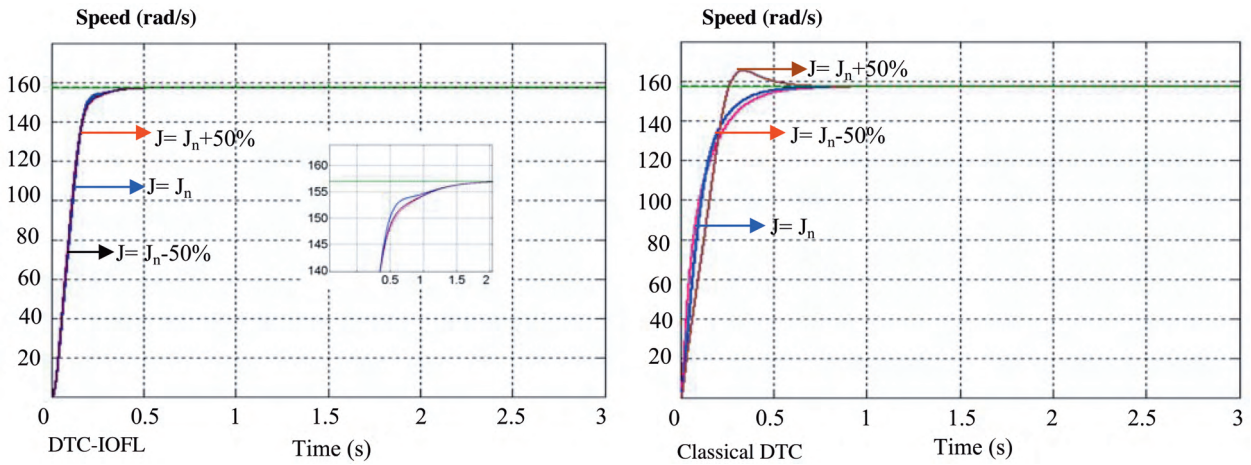

Figure 8. Drive response under different inertia values.

8. Conclusion

We presented a robust DTC method for a voltage inverter-fed IM based on a SVPWM scheme combined with the IOFL technique.

The overall torque and flux control system was verified to be robust to the variations of motor mechanical and electrical parameter variations. Simulation studies were used to demonstrate the characteristics of the proposed method. It was shown that the proposed IOFL controller has better tracking performance and robustness against parameters variations as compared with the conventional DTC.

References

[1] I. Takahashi, T. Noguchi, "A new quick-response and high-efficiency control strategy of an induction machine", IEEE Transactions on Industry Applications, Vol. 22, pp. 820-827, 1986.

[2] S. Belkacem, F. Naceri, R. Abdessemed, "A novel robust adaptive control algorithm and application to DTC-SVM of AC drives", Serbian Journal of Electrical Engineering, Vol. 7, pp. 21-40, 2010.

[3] Y. Kumsuwan ,W. Srirattanawichaikul, S. Premrudeepreechacharn, "Reduction of torque ripple in direct torque control for induction motor drives using decoupled amplitude and angle of stator flux control", ECTI Transactions on Electrical Engineering, Electronics and Communications, Vol. 8, pp. 187-196, 2010.

[4] Z. Zhang, R. Tang, B. Bai, D. Xie, "Novel direct torque control based on space vector modulation with adaptive stator flux observer for induction motors", IEEE Transactions on Magnetics, Vol. 46, pp. 3133-3136, 2010.

[5] G.R. Arab Markadeh, J. Soltani, "Robust direct torque and flux control of adjustable speed sensorless induction machine drive based on space vector modulation using a PI predictive controller", Electrical Engineering, Vol. 88, pp. 485-496, 2006.

[6] M. Romero, J.H. Braslavsky, M.I. Valla, "Ripple reduction in direct torque and flux control of induction motors via sliding modes", Latin American Applied Research, Vol. 37, pp. 289-297, 2007.

[7] C. Bharatiraja, S. Jeevananthan, R. Latha, "A novel space vector pulse width modulation based high performance variable structure direct torque control evaluation of induction machine drives", International Journal of Computer Applications, Vol. 3, pp. 33-38, 2010.

[8] N. Taib, T. Rekioua, B. Francois, "An improved fixed switching frequency direct torque control of induction motor drives fed by direct matrix converter", International Journal of Computer Science and Information Security, Vol. 7, pp. 198-205, 2010.

[9] H. Li, Q. Mo, Z. Zhao, "Research on direct torque control of induction motor based on genetic algorithm and fuzzy adaptive PI controller", Measuring Technology and Mechatronics Automation, Vol. 3, pp. 46-49, 2010.

[10] S.X. Liu, M.Y. Wang, Y.G. Chen, S. Li, "A novel fuzzy direct torque control system for three-level inverter-fed induction machine", International Journal of Automation and Computing, Vol. 7, pp. 78-85, 2010.

[11] Z. Jiang, S. Hu, W. Cao, "A new fuzzy logic torque control scheme based on vector control and direct torque control for induction machine", Proceedings of the 3rd International Conference on Innovative Computing Information and Control, p. 500, 2008.

[12] T. Riad, B. Hocine, M. Salima, "New direct torque neuro-fuzzy control based SVM-three level inverter-fed induction motor", International Journal of Control, Automation, and Systems, Vol. 8, pp. 425-432, 2010.

[13] S. Belkacem, F. Naceri, R. Abdessemed, "Robust nonlinear control for direct torque control of induction motor drive using space vector modulation", Journal of Electrical Engineering, Vol. 10, pp. 79-87, 2010.

[14] M. Hajian, J. Soltani, G. Arab Markadeh, S. Hosseinnia, "Adaptive nonlinear direct torque control of sensorless IM drives with efficiency optimization", IEEE Transactions on Industrial Electronics, Vol. 57, pp. 975-958, 2010.

[15] M. Hajian, J. Soltani, G.R. Arab Markadeh, S. Hosseinnia, "Input-output feedback linearization of sensorless IM drives with stator and rotor resistances estimation", Journal of Power Electronics, Vol. 9, pp. 654-666, 2009.

[16] H. Abootorabi Zarchi, G.R. Arab Markadeh, J. Soltani, "Direct torque and flux regulation of synchronous reluctance motor drives based on input-output feedback linearization", Energy Conversion and Management, Vol. 51, pp. 71-80, 2010.

[17] S. Belkacem, B. Zegueb, F. Naceri, "Robust non-linear direct torque and flux control of adjustable speed sensorless PMSM drive based on SVM using a PI predictive controller", Journal of Engineering Science and Technology Review, Vol. 3, pp. 168-175, 2010.

[18] J.J.E Slotine, W. Li, Applied Nonlinear Control, New Jersey, Prentice-Hall, 1991.

[19] A. Isidori, Nonlinear Control Systems, 2nd ed., New York, Springer, 1989.

[20] J. Chiasson, "Dynamic feedback linearization of the induction motor", IEEE Transactions on Automatic Control, Vol. 38, pp. 1588-1594, 1993.

[21] R. Marino, P. Tomei, C.M. Verrelli, "An adaptive tracking control from current measurements for induction motors with uncertain load torque and rotor resistance", Automatica Journal, Vol. 44, pp. 2593-2599, 2008.

[22] B.M. Dehkordi, A.F. Payam, M.N. Hashemnia, S.K. Sul, "Design of an adaptive backstepping controller for doubly-fed induction machine drives", Journal of Power Electronics, Vol. 9, pp. 343-353, 2009.

[23] R. Marino, P. Tomei, C.M. Verrelli, "Adaptive output feedback tracking control for induction motors with uncertain load torque and resistances", International Symposium on Power Electronics Electrical Drives Automation and Motion, pp. 419-424, 2010.

[24] S. Belkacem, F. Naceri, R. Abdessemed, "A new control strategy by combining direct torque control with feedback linearization for induction motor drive", 11th International Conference on Sciences and Techniques of Automatic Control and Computer Engineering, 2010.